MOLECULAR AND CELLULAR BIOLOGY, July 2002, p. 4567–4578 Vol. 22, No. 13
0270-7306/02/$04.00+0 DOI: 10.1128/MCB.22.13.4567–4578.2002

SOCS-6 Binds to Insulin Receptor Substrate 4, and Mice Lacking the SOCS-6 Gene Exhibit Mild Growth Retardation

Danielle L. Krebs,[1]* Rachel T. Uren,[1] Donald Metcalf,[1] Steven Rakar,[1] Jian-Guo Zhang,[1] Robyn Starr,[1] David P. De Souza,[1] Kathy Hanzinikolas,[1] Jo Eyles,[1] Lisa M. Connolly,[2] Richard J. Simpson,[2] Nicos A. Nicola,[1] Sandra E. Nicholson,[1] Manuel Baca,[1] Douglas J. Hilton,[1] and Warren S. Alexander[1]

The Walter and Eliza Hall Institute of Medical Research and the Cooperative Research Centre for Cellular Growth Factors[1] and Joint Protein Structure Laboratory of the Walter and Eliza Hall Institute and Ludwig Institute for Cancer Research,[2] Royal Melbourne Hospital, Victoria 3050, Australia

Received 25 October 2001/Returned for modification 11 December 2001/Accepted 2 April 2002

SOCS-6 is a member of the suppressor of cytokine signaling (SOCS) family of proteins (SOCS-1 to SOCS-7 and CIS) which each contain a central SH2 domain and a carboxyl-terminal SOCS box. SOCS-1, SOCS-2, SOCS-3, and CIS act to negatively regulate cytokine-induced signaling pathways; however, the actions of SOCS-4, SOCS-5, SOCS-6, and SOCS-7 remain less clear. Here we have used both biochemical and genetic approaches to examine the action of SOCS-6. We found that SOCS-6 and SOCS-7 are expressed ubiquitously in murine tissues. Like other SOCS family members, SOCS-6 binds to elongins B and C through its SOCS box, suggesting that it might act as an E3 ubiquitin ligase that targets proteins bound to its SH2 domain for ubiquitination and proteasomal degradation. We investigated the binding specificity of the SOCS-6 and SOCS-7 SH2 domains and found that they preferentially bound to phosphopeptides containing a valine in the phosphotyrosine (pY) +1 position and a hydrophobic residue in the pY +2 and pY +3 positions. In addition, these SH2 domains interacted with a protein complex consisting of insulin receptor substrate 4 (IRS-4), IRS-2, and the p85 regulatory subunit of phosphatidylinositol 3-kinase. To investigate the physiological role of SOCS-6, we generated mice lacking the SOCS-6 gene. SOCS-6$^{-/-}$ mice were born in a normal Mendelian ratio, were fertile, developed normally, and did not exhibit defects in hematopoiesis or glucose homeostasis. However, both male and female SOCS-6$^{-/-}$ mice weighed approximately 10% less than wild-type littermates.

The suppressor of cytokine signaling (SOCS) family contains eight proteins, SOCS-1 to SOCS-7 and CIS, which are characterized by an amino-terminal (N-terminal) region of variable length, a central SH2 domain, and a carboxyl-terminal (C-terminal) SOCS box (22). CIS, SOCS-1, SOCS-2, and SOCS-3 are generally present in cells at low levels, but their transcription is rapidly upregulated in response to stimulation by a wide range of cytokines, growth factors, and hormones (38). When overexpressed in cell lines, CIS, SOCS-1, and SOCS-3 potently inhibit signaling by a large variety of stimuli, including interleukin-2 (IL-2), IL-3, prolactin, growth hormone (GH), and erythropoietin (22). These SOCS family members therefore appear to act in part of a classical negative feedback loop, inhibiting the signaling pathways that initially led to their production.

The broad range of action exhibited by SOCS-1 and SOCS-3 is likely due to their ability, either directly or indirectly, to inhibit the catalytic activity of the Janus kinases (JAKs), which play an essential role in virtually all cytokine-induced signaling pathways (7, 14, 31, 36, 41). In contrast, CIS appears to modulate signaling by competing with STATs for binding sites on activated cytokine receptors (33, 42). SOCS-2 weakly inhibits signaling by prolactin, GH, and insulin-like growth factor 1 (IGF-1) in vitro but is a significantly less potent inhibitor than CIS, SOCS-1, or SOCS-3, and its mode of action remains to be determined (32, 34, 44).

Mice lacking SOCS-1, SOCS-2, or SOCS-3 have been studied in order to elucidate their physiological action. Mice lacking SOCS-1 die neonatally of a disease characterized by severe lymphopenia, fatty degeneration of the liver, activation of T cells, and hematopoietic infiltration of multiple organs (30, 37). This syndrome appears to be caused by excessive gamma interferon production and signaling, suggesting that SOCS-1 is a key negative regulator of gamma interferon action in vivo (2, 24). Mice lacking SOCS-2 are significantly larger than wild-type littermates, a phenotype likely caused by dysregulation of the IGF-1–GH axis (27). Mice lacking SOCS-3 die in utero as a result of placental insufficiency, although the signaling pathways presumed to be dysregulated in these mice have not yet been identified (23, 35).

Recent studies have shed light on the function of the SOCS box. In a screen to identify proteins that interact with the SOCS box, it was discovered that elongins B and C are prominent binding partners (18, 43). The elongin B/C complex in turn binds to cullin2 or cullin5 and Rbx1, to form a multiprotein complex capable of E3 ubiquitin ligase activity (17). In light of this, we and others hypothesized that SOCS proteins might act as adapters that link the proteins bound to their SH2 domains to the ubiquitination machinery. Indeed, SOCS-1 binds to Tel-Jak2 through its SH2 domain and in doing so facilitates Tel-Jak2 ubiquitination and proteasomal degrada-

* Corresponding author. Mailing address: The Walter and Eliza Hall Institute of Medical Research, Post Office, Royal Melbourne Hospital, Victoria 3050, Australia. Phone: 61-3-9345-2525. Fax: 61-3-9345-2616. E-mail: krebs@wehi.edu.au.

tion (11, 16, 28). In addition, the ubiquitination and degradation of Tel-Jak2 occur in a SOCS box-dependent manner (11, 16). SOCS-1 also constitutively binds to the guanine nucleotide exchange factor Vav, and when coexpressed, SOCS-1 stimulates the ubiquitination and degradation of Vav (8). Interestingly, some studies suggest that the interaction between the SOCS box and elongins B and C acts to stabilize SOCS proteins, although the mechanism by which stabilization occurs remains unclear (13, 18).

Unlike CIS and SOCS-1 to -3, SOCS-4 to -7 have been less extensively studied. SOCS-6 and SOCS-7 share 56% amino acid identity in their SH2 domain and 53% in their SOCS box, making them more similar to each other than to other SOCS family members. SOCS-6 and SOCS-7 contain relatively large N-terminal domains, of more than 350 amino acids, and while the SOCS-6 N-terminal domain contains no identifiable protein interaction motifs, the SOCS-7 N-terminal domain contains a putative nuclear localization signal and multiple proline-rich regions (26). In contrast to SOCS-1 and SOCS-3, SOCS-6 and SOCS-7 do not contain the "extended SH2 subdomain" motif (41) which facilitates high-affinity binding to phosphotyrosine. Unlike other SOCS family members, SOCS-6 does not interact with JAK2 (25) or inhibit signaling by GH, leukemia inhibitory factor, or prolactin (15, 31, 34). However, SOCS-6 binds to the insulin receptor in response to insulin treatment and inhibits downstream signaling events, such as the activation of ERK1/2, Akt, and insulin receptor substrate 1 (IRS-1) (29).

Here, we have used biochemical and genetic approaches to explore the action of SOCS-6. We show that SOCS-6 is a ubiquitously expressed protein that binds to elongins B and C via the SOCS box domain. We defined the SOCS-6 and SOCS-7 SH2 domain binding specificity and found that these SH2 domains bind to IRS-4, IRS-2, and the p85 subunit of phosphatidylinositol 3-kinase (PI3K). To investigate the biological function of SOCS-6, we have generated mice that lack the SOCS-6 gene. SOCS-$6^{-/-}$ mice develop normally but grow to a size 8 to 10% smaller than wild-type littermates.

MATERIALS AND METHODS

Antibodies. Anti-SOCS-6 monoclonal antibodies were produced by immunizing mice with a protein consisting of glutathione *S*-transferase fused to amino acids 180 to 380 of murine SOCS-6 (the region immediately prior to the SH2 domain). Three anti-SOCS-6 monoclonal antibodies, 1C1, 1C3, and 3A7, recognized SOCS-6 in both immunoprecipitates and Western blots. The epitopes recognized by these antibodies were mapped to within 40 amino acids by determining their reactivity with progressively truncated versions of the SOCS-6 N-terminal domain expressed in 293T cells. Both 1C1 and 1C3 recognized epitopes lying between amino acids 260 and 299, while 3A7 recognized an epitope lying between amino acids 300 and 339 (data not shown). Antiphosphotyrosine (clone 4G10), anti-p85, and anti-IRS-4 antibodies were from Upstate Biotechnology, Lake Placid, N.Y.; M2 anti-FLAG resin was from Sigma, Castle Hill, New South Wales, Australia; sheep anti-mouse immunoglobulin G (IgG)–horseradish peroxidase (HRP) antibodies were from Amersham Pharmacia, Sydney, New South Wales, Australia; goat anti-rabbit IgG–HRP antibodies were from Bio-Rad, Hercules, Calif.; goat anti-rat IgM/IgG–HRP antibodies were from Southern Biotechnology, Birmingham, Ala. The anti-elongin B/C antibodies and the rat anti-FLAG antibodies were gifts from J.-G. Zhang and A. Strasser, respectively, from the Walter and Eliza Hall Institute of Medical Research. The anti-heat shock protein 70 antibody was a gift from R. Anderson, Peter MacCallum Cancer Institute, Melbourne, Australia.

Cloning and targeting the murine SOCS-6 gene. A phage library of 129/Sv mouse genomic clones (λFIXII; Stratagene, La Jolla, Calif.) was screened with oligonucleotides corresponding to the murine SOCS-6 coding sequence. Clones hybridizing with these probes were purified and analyzed by DNA sequencing and restriction endonuclease mapping using standard techniques. The PCR was used to generate a 2.3-kbp fragment extending 5′ from the SOCS-6 ATG initiation codon. This fragment was fused to the ATG of *lacZ* by ligation into the *Bam*HI site in the plasmid vector pβgalpAloxneo (37). A 4.0-kbp 3′ SOCS-6 fragment engineered to have *Xho*I sites at both termini was generated by PCR and ligated into the *Xho*I site of the pβgalpAloxneo plasmid containing the 5′ SOCS-6 arm (see Fig. 5A). This targeting vector was linearized with *Not*I and electroporated into C57BL/6 embryonic stem (ES) cells (21). ES cells were then selected in 175 μg of G418 per ml, and resistant clones were screened by Southern blot analysis by probing *Eco*RV-digested genomic DNA with either a 0.2-kbp *Xba*I-*Kpn*I fragment or a 1.2-kbp *Xba*I-*Spe*I fragment located upstream of the 5′ arm. This strategy provided distinction between the endogenous (18-kbp) and targeted (5.5-kbp) SOCS-6 alleles. Two independent ES cell clones harboring the targeted SOCS-6 gene were injected into BALB/c blastocysts to generate chimeric mice. Male chimeras were mated with C57BL/6 females to yield heterozygotes for the targeted SOCS-6 allele, and these were then interbred to produce wild-type (SOCS-$6^{+/+}$), heterozygous (SOCS-$6^{+/-}$), and mutant (SOCS-$6^{-/-}$) mice on a pure C57BL/6 genetic background. The SOCS-$6^{-/-}$ strain was then maintained by intercrossing SOCS-$6^{-/-}$ mice.

Nucleic acid analysis. Extraction of genomic DNA from tail tips, analysis by Southern blot, and the purification of poly(A)$^+$ RNA for Northern blot analysis were performed essentially as previously described (1). The SOCS-6 cDNA probe used for Northern blot hybridization was a 920-bp *Pst*I fragment which spanned nucleotides 574 to 1495 in the SOCS-6 coding sequence. The SOCS-7 cDNA probe used for Northern blot hybridization was a 1.3-kbp *Eco*RI-*Xho*I fragment. The glyceraldehyde-3-phosphate dehydrogenase (GAPDH) cDNA probe used for Northern blot analysis was a 1.2-kbp *Pst*I fragment.

Preparation of SOCS-6 and SOCS-7 SH2 domain affinity resins. Fragments of the murine SOCS-6 and SOCS-7 proteins encompassing the SH2 domains were expressed in *Escherichia coli* as hexahistidine-tagged proteins. The recombinant proteins were purified from bacterial cells lysed in 7 M guanidinium hydrochloride using immobilized metal affinity chromatography. Purified proteins were refolded by dialysis against mouse tonicity phosphate-buffered saline (MT-PBS) containing 0.02% (vol/vol) Tween 20 and 0.5 mM Tris(2 carboxyethyl)-phosphine hydrochloride and covalently immobilized on *N*-hydroxysuccinimide (NHS)-activated Sepharose at a density of 3 mg of protein per ml of resin. Control resin was prepared by derivatizing NHS-activated Sepharose resin with ethanolamine.

Synthesis and screening of phosphopeptide libraries. A partially degenerate phosphopeptide library, VE(pY)XXXVHSGR, where pY represents phosphotyrosine and X is an equal mixture of all possible L-amino acids with the exception of cysteine, was synthesized to probe the ligand binding specificity of the SH2 domains from SOCS-6 and SOCS-7. The invariable portion of the library was synthesized by using standard 9-fluorenylmethoxy carbonyl-based solid-phase peptide synthesis protocols, while the randomized positions were generated by a split-and-pool strategy. Following peptide cleavage and deprotection, the correct sequence and equal distribution of each amino acid at the randomized positions were confirmed by N-terminal sequencing. To screen for SH2-binding peptides, 400-μl aliquots of immobilized protein resins were incubated for 1 h at room temperature with 4 mg of phosphopeptide library solubilized in 2 ml of 50 mM sodium phosphate (pH 7.5) containing 150 mM NaCl, 2 mM dithiothreitol, and 0.2% (vol/vol) Tween 20. After the resins had been washed five times with 8 ml of MT-PBS containing 0.2% (vol/vol) Tween 20 and once with 8 ml of 2 mM sodium phosphate (pH 7.5), bound phosphopeptides were eluted with 1% (vol/vol) aqueous trifluoroacetic acid (TFA) and lyophilized. A control experiment was performed in the same way with control resin in place of the SH2 protein resin. The dried samples were resuspended in aqueous TFA-acetonitrile and sequenced on an Applied Biosystems 494 Procise protein sequencer. The enrichment value was calculated for each random position by dividing the amount of each amino acid at a given cycle of the SH2 resin experiment by the amount of the same amino acid in the same cycle of the control experiment. Enrichment values were scaled so that the sum of all values is equal to the total number of amino acids in the degenerate position (i.e., 19).

Cell maintenance and transfection. The 293T human fibroblast and M1 myeloid leukemia cell lines were grown in Dulbecco's modified Eagle medium (DME) supplemented with 10% (vol/vol) fetal bovine serum. 293T cells were transfected with 0.75 to 2.5 μg of the pEF-FLAG-I expression vector (31) containing the cDNA of interest, using the FuGENE 6 transfection reagent (Roche, Indianapolis, Ind.), according to the manufacturer's instructions. Cells were analyzed 48 h posttransfection.

Preparation of protein lysates. Tissues were dissected from mice and immediately frozen in liquid nitrogen. Frozen tissues were then pulverized and extracted by Dounce homogenization in KALB lysis buffer (150 mM NaCl, 50 mM Tris [pH 7.5], 1% [vol/vol] Triton X-100, 1 mM EDTA, 1 mM Na_3VO_4, 1 mM

NaF) containing protease inhibitors (Complete cocktail tablets; Roche). For stimulations, 293T cells were starved overnight in DME containing 0.5% (vol/vol) serum and stimulated with either 100 ng of rat IGF-1 (GroPep, Adelaide, South Australia) per ml, 100 nM insulin (Sigma), or 50% (vol/vol) serum for 15 to 20 min. 293T cells were then washed with ice-cold MT-PBS and extracted in KALB buffer plus inhibitors. For experiments shown in Fig. 4B and C, cells were lysed in RIPA buffer (1% [vol/vol] Triton X-100, 1% deoxycholate, 0.1% [wt/vol] sodium dodecyl sulfate [SDS], 144 mM NaCl, 10 mM Tris [pH 7.5], 1 mM Na_3VO_4, 1 mM NaF) containing protease inhibitors, and DNA was sheared by passage through a 25-gauge needle. M1 cells were washed with ice-cold MT-PBS and then extracted in KALB buffer plus inhibitors at a concentration of 10^8 cells/ml. In all cases, insoluble material was removed by centrifugation and protein concentrations were determined using the Coomassie protein assay reagent (Pierce, Rockford, Ill.).

Immunoprecipitations. Lysate from 1×10^6 to 4×10^6 293T cells, 15 mg of murine tissue lysate, or 3×10^8 M1 cells was precleared with 20 μl of protein A-Sepharose for 30 min at 4°C. Lysates were then transferred to a new tube and mixed with 1 to 4 μg of primary antibody plus 25 μl of protein A-Sepharose, for 3 h at 4°C. Immune complexes were collected by adding 25 μl of protein A-Sepharose and mixing for 1 h. Alternatively, precleared lysates were mixed with 10 μl of M2 anti-FLAG resin for 3 h. For small-scale SOCS-6 and SOCS-7 SH2 domain precipitations, precleared lysates were added to 5 μl of SH2 resin plus 20 μl of protein A-Sepharose and mixed for 3 h. Beads were washed three to six times in KALB lysis buffer containing protease inhibitors, and bound proteins were eluted by boiling for 5 min in reducing SDS-polyacrylamide gel electrophoresis (PAGE) sample buffer.

Western blotting. Proteins were separated on SDS-PAGE gels and transferred to polyvinylidene difluoride membranes (PVDF-Plus; Micron Separations Inc., Westborough, Mass.). Filters were blocked for 1 h in 10% (wt/vol) milk powder in MT-PBS, except antiphosphotyrosine blots, which were blocked in 1% (wt/vol) bovine serum albumin in MT-PBS. Primary antibodies were diluted in MT-PBS containing 1% (wt/vol) bovine serum albumin and 0.1% (vol/vol) Tween 20 and were incubated with the filter for 3 h at room temperature. Secondary antibodies were added for 1 h in the same solution. Blots were stripped by incubation in 62.5 mM Tris-HCl (pH 6.7), 2% (wt/vol) SDS, and 100 mM 2-mercaptoethanol for 5 min at 50°C.

Large-scale purification of proteins bound to the SOCS-6 and SOCS-7 SH2 domains. Lysate from approximately 6×10^8 293T cells was precleared with 200 μl of protein A-Sepharose for 30 min at 4°C. Lysates were then transferred to a new tube and mixed with 50 μl of SOCS-6 SH2 resin, SOCS-7 SH2 resin, or control resin for 3 h at 4°C. The beads were then washed eight or nine times in KALB lysis buffer containing protease inhibitors, and bound proteins were eluted by boiling for 10 min in reducing SDS-PAGE sample buffer. Proteins were separated on an SDS–8% PAGE gel and visualized by Coomassie blue staining. Bands of interest were then excised and subjected to mass-spectrometric analysis.

Protein identification by peptide sequence analysis using tandem mass spectrometry. Mass spectrometric analysis was carried out as described previously (43). Briefly, proteins were excised from gels and digested in situ with trypsin. Peptides were then separated by capillary chromatography and sequenced with an on-line electrospray ion-trap mass spectrometer (LCQ Finnigan-MAT, San Jose, Calif.). Peptide sequences were identified manually or by using the SEQUEST algorithm to correlate the collision-induced dissociation spectra with amino acid sequences in the OWL protein database (version 30.2).

Histological analysis. Tissues (uterus, bladder, liver, testes, seminal vesicles, skin, eye, kidney, heart, lung, thymus, salivary gland, small intestine, muscle, brain, spleen, and pancreas) were fixed in 10% buffered formalin and embedded in paraffin. Sections were then prepared, stained with hematoxylin and eosin, and examined by light microscopy.

Hematological analysis. Peripheral white blood cell and platelet counts were determined manually. Single-cell suspensions from femoral bone marrow, spleen, liver, and peritoneum were prepared by standard techniques, and differential cell counts were performed on smears or cytocentrifuge preparations stained with May-Grunwald-Giemsa stain. Analysis of agar cultures was carried out essentially as described previously (20). Briefly, colony formation was stimulated by the addition of serial dilutions of either granulocyte-macrophage colony-stimulating factor (GM-CSF), macrophage CSF, granulocyte CSF (G-CSF), IL-3, or stem cell factor (SCF). After 7 days in a humidified atmosphere of 10% CO_2, cultures were scored manually and then fixed in 1 ml of 2.5% glutaraldehyde. Following this, cultures were transferred onto glass slides and stained with acetylcholinesterase and then with Luxol Fast Blue (BDH Laboratory, Poole, United Kingdom) and hematoxylin. Cultures were analyzed manually to determine the number and composition of colonies within the cultures.

Flow cytometry. Single-cell suspensions of bone marrow cells, splenocytes, and thymocytes from 8- to 12-week-old SOCS-$6^{-/-}$ mice and normal littermates were prepared. Erythrocytes were lysed, and the cells were stained with rat monoclonal antibodies for specific cell surface markers and analyzed by flow cytometry as previously described (39). The FACSgal assay (10) was used to detect transcription of the β-galactosidase gene under the control of the SOCS-6 promoter. Briefly, bone marrow cells were loaded by incubation with an equal volume of 2 mM fluorescein-di-β-D-galactopyranoside under hypotonic conditions for 2 min at 37°C, immediately placed on ice, and then incubated on ice for 3 h prior to analysis. Cells were then sorted into fractions expressing high, intermediate, and low levels of β-galactosidase and analyzed for colony formation in response to GM-CSF, IL-3, or G-CSF plus SCF, as described above. In all cases, cells were analyzed and/or sorted using FACStar Plus (Becton Dickinson, San Jose, Calif.), excluding dead cells with propidium iodide staining.

Blood glucose and plasma insulin concentrations. To determine basal blood glucose concentrations, male age-matched mice fasted overnight or were fed ad libitum and then bled for total blood or preparation of plasma. All blood glucose concentrations were determined with an Advantage glucometer and Advantage II glucose blood test strips (Roche). Plasma insulin concentrations were determined with a sensitive rat insulin radioimmunoassay (Linko, St. Charles, Mo.).

Glucose and insulin tolerance tests. For glucose tolerance, male age-matched mice fasted overnight and then were given an intraperitoneal injection of 1.2 g of D-glucose per kg of body weight, in a solution of 0.25 g/ml. For insulin tolerance, age-matched male mice fasted overnight and were then given an intraperitoneal injection of 0.75 U of insulin per kg of body weight, in a solution of 0.25 U/ml. Blood was then collected from the orbital sinus of anesthetized mice at regular intervals, and glucose concentrations were determined as described above.

RESULTS

SOCS-6 binds to elongins B and C through its SOCS box. In order to begin to assess the function of SOCS-6, we sought to determine the proteins with which it interacts. We have previously shown that in M1 cells, both SOCS-1 and SOCS-3 constitutively associate with the elongin B/C complex in a SOCS box-dependent manner (43). To determine whether SOCS-6 also binds to elongins B and C, M1 cell lysates were subjected to immunoprecipitation with anti-SOCS-6 antibodies followed by Western blotting with polyclonal antibodies that recognize both elongins B and C. Elongins B and C were detected in the anti-SOCS-6 immunoprecipitate but not in the isotype-matched control immunoprecipitate, demonstrating that endogenous SOCS-6 binds to elongins B and C in M1 cells (Fig. 1A). To investigate whether this interaction occurs through the SOCS-6 SOCS box, four N-terminal FLAG epitope-tagged versions of SOCS-6 (SOCS-6 N-terminal region [N], SOCS-6 N-terminal region and SH2 domain [N+SH2], SOCS-6 SH2 domain and SOCS box [SH2+SB], and the full-length SOCS-6 protein [FLAG-S6]) were expressed in 293T cells. Cell lysates were immunoprecipitated with anti-FLAG antibodies and then Western blotted with antibodies that recognize both elongins B and C. Endogenous elongins B and C bound to the FLAG-S6 and SH2+SB proteins but not to the N or N+SH2 proteins (Fig. 1B). Thus, like SOCS-1 and SOCS-3, SOCS-6 associates with elongins B and C in a SOCS box-dependent manner.

Determination of the SOCS-6 and SOCS-7 SH2 domain binding specificity. SH2 domain-containing proteins typically act to regulate signal transduction pathways by binding to a small number of tyrosine-phosphorylated proteins. We therefore aimed to elucidate the signaling pathways that might be regulated by SOCS-6 and SOCS-7 by identifying proteins that interacted with their SH2 domains. We first determined the spectrum of proteins that might interact with the SOCS-6 and SOCS-7 SH2 domains by using these domains to screen synthetic phosphopeptide libraries. We found that the phos-

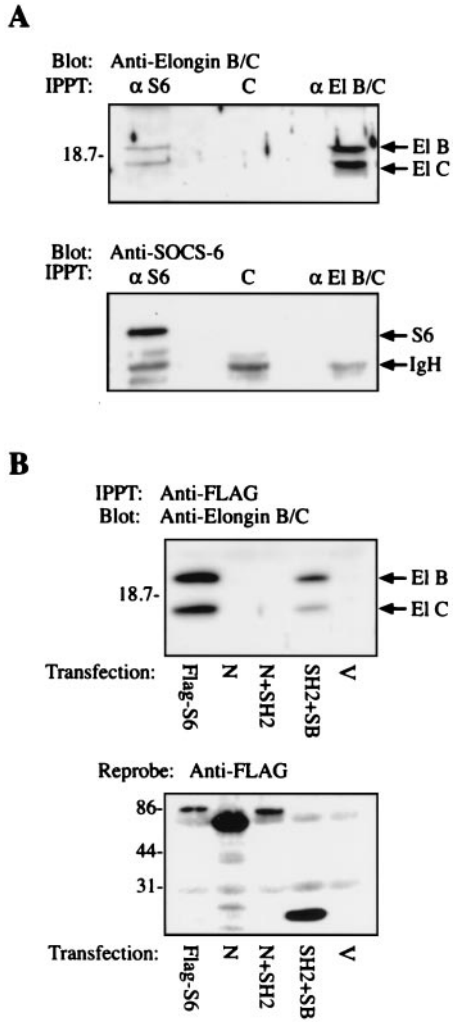

FIG. 1. SOCS-6 associates with elongins B and C. (A) Endogenous SOCS-6 binds to endogenous elongins B and C. M1 cells were lysed and subjected to immunoprecipitation with either the 1C3 anti-SOCS-6 antibody, a control isotype matched (IgG2B) antibody, or a monoclonal antibody that recognizes both elongins B and C. This was followed by Western blotting with the polyclonal antibody that recognizes both elongins B and C (top). To confirm that SOCS-6 was immunoprecipitated, 1/10 of each immunoprecipitate was subjected to Western blotting with the 3A7 anti-SOCS-6 antibody (bottom). (B) SOCS-6 binds to elongins B and C through its SOCS box. 293T cells were transfected with cDNAs encoding FLAG-S6, N, N+SH2, or SH2+SB proteins or with the empty vector (V). Lysates were prepared and subjected to immunoprecipitation using M2 anti-FLAG resin followed by Western blotting with a polyclonal antibody that recognizes both elongins B and C (top). The filter was then stripped and reprobed with anti-FLAG antibodies (bottom). Molecular masses (kilodaltons) are on the left. IPPT, immunoprecipitate; S6, SOCS-6; El, elongin; C, control antibody; IgH, immunoglobulin heavy chain.

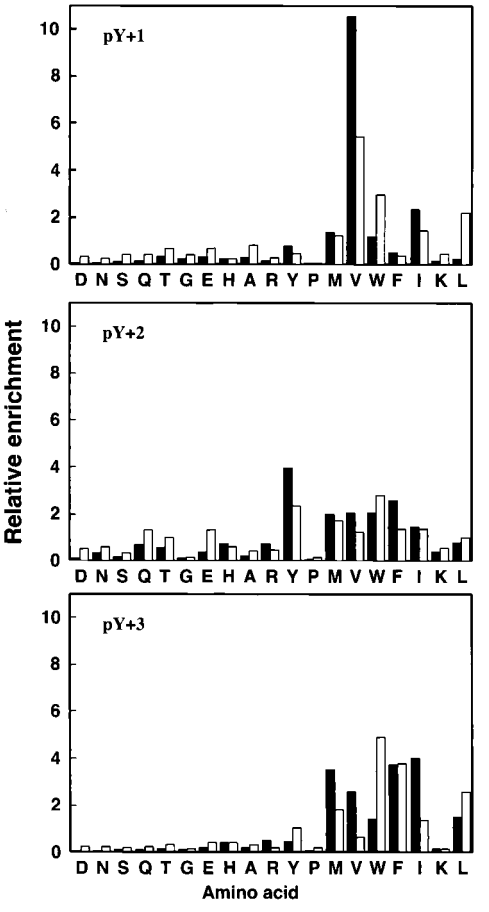

FIG. 2. Selection of phosphopeptides that bind the SOCS-6 and SOCS-7 SH2 domains. The degenerate phosphopeptide library VEpYXXXVHSGR was incubated with Sepharose resin containing either immobilized SOCS-6 or SOCS-7 SH2 domain. The column was washed, and bound peptides were eluted with 1% (vol/vol) aqueous TFA. The eluted peptide mixture was analyzed by N-terminal sequencing, and the results were compared to those from the eluate of Sepharose resin alone. Data is shown for the relative amino acid composition at each of the randomized positions within the phosphopeptide mixtures eluted from the SOCS-6 (filled bars) and SOCS-7 (open bars) SH2 domain resins. The data have been normalized so that the sum of the values of all amino acids equals the number of amino acids (i.e., 19).

phopeptide binding preferences of the two proteins were quite similar, suggesting that the primary sequence similarity of SOCS-6 and SOCS-7 extends to their capacity to recognize the same cellular phosphorylated proteins. Phosphopeptides containing a valine in the pY +1 position (i.e., the first amino acid downstream from the phosphotyrosine residue) were highly selected, as were phosphopeptides containing a hydrophobic residue at pY +3. Some preference for hydrophobic residues at pY +2 was also evident (Fig. 2). We found that the phosphotyrosine binding motifs favored by the SOCS-3 and SHP-2 SH2 domains differed significantly from the motif favored by the SOCS-6 and SOCS-7 SH2 domains (M. Baca et al., unpublished data), indicating that the binding of phosphopeptides to the SOCS-6 and SOCS-7 SH2 domains was specific.

Identification of proteins that bind to the SOCS-6 and SOCS-7 SH2 domains. We next tested whether tyrosine-phosphorylated proteins bound to the SOCS-6 or SOCS-7 SH2 domain by incubating lysates derived from 293T cells with the SOCS-6 and SOCS-7 SH2 domains immobilized to resin. Although no tyrosine-phosphorylated proteins in lysates derived from unstimulated cells bound, prominent tyrosine-phosphorylated proteins with apparent molecular weights of 90,000 and

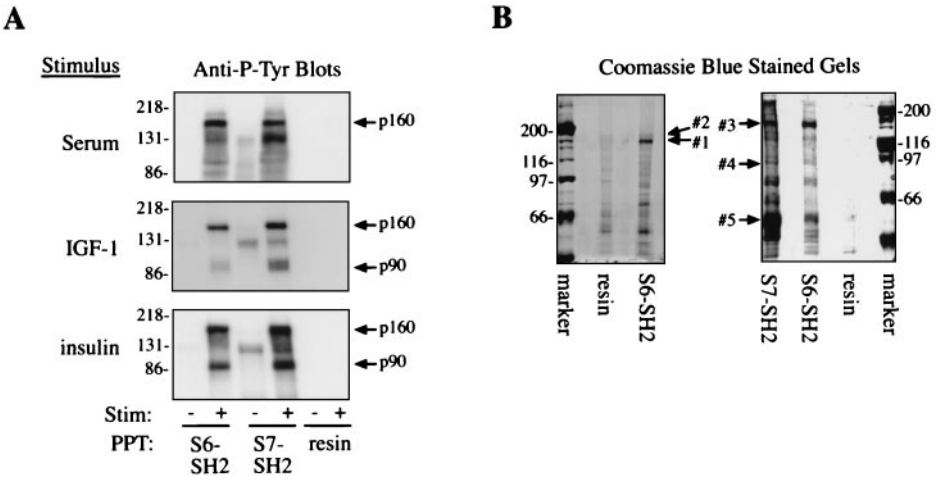

FIG. 3. Identification of proteins that bind to the SOCS-6 and SOCS-7 SH2 domains. (A) 293T cells were either left unstimulated (−) or stimulated (+) with 50% (vol/vol) serum, 100 nM insulin, or 100 ng of IGF-1 per ml for 15 min. Lysates were subjected to precipitation with either SOCS-6 SH2 resin, SOCS-7 SH2 resin, or control resin, and precipitates were immunoblotted with antiphosphotyrosine antibodies (anti-P-Tyr). (B) Lysate from approximately 6×10^8 293T cells was subjected to precipitation with either SOCS-6 SH2 resin, SOCS-7 SH2 resin, or control resin. Bound proteins were separated on SDS-PAGE gels and visualized by Coomassie blue staining. Bands of interest were then excised, and proteins were identified by mass spectrometry. Molecular mass (in kilodaltons) is indicated. Stim, stimulation; PPT, precipitate.

160,000 bound to both the SOCS-6 and SOCS-7 SH2 domains in lysates derived from cells that were stimulated with serum, insulin, or IGF-1 (Fig. 3A).

To identify these associated proteins, we used the SOCS-6 and SOCS-7 SH2 domains as affinity resins to purify proteins from lysates derived from 6×10^8 IGF-1-stimulated 293T cells. The precipitates were separated on SDS-PAGE gels, and proteins were visualized by Coomassie blue staining. Proteins that bound to the SOCS-6 and SOCS-7 SH2 domains but not to control resin were excised from the gels, digested with trypsin and analyzed by mass spectrometry. This included the proteins with apparent molecular weights of 90,000 and 160,000, presumed to correspond to the phosphoproteins identified above, as well as proteins with apparent molecular weights of 85,000 and 50,000 (Fig. 3B). The identity of these proteins was then determined by mass-spectrometric analysis (Table 1).

The protein with an apparent molecular weight of 160,000 proved to include a mixture of IRS-4 (bands 1 and 3) and IRS-2 (band 2), both of which are known to be tyrosine phosphorylated in response to insulin and IGF-1 (4, 12), and the 90,000-molecular-weight protein was identified as a degradation product of IRS-4 (band 4). Thus, IRS-4 appeared to be the primary tyrosine-phosphorylated protein that bound to the SOCS-6 and SOCS-7 SH2 domains in IGF-1-stimulated 293T cells. Other proteins that bound to the SOCS-6 and SOCS-7 SH2 domains were identified as the p85 (α and β) regulatory subunit of PI3K (band 4) and tubulin (band 5). The latter is found associated with many different proteins in pull-down experiments and is likely to be nonspecific.

We confirmed that the SOCS-6 and SOCS-7 SH2 domains bound to IRS-4 and p85 in response to IGF-1 stimulation by subjecting unstimulated and IGF-1-stimulated cell lysates to precipitation with the SOCS-6 or SOCS-7 SH2 domains and then immunoblotting with antibodies that specifically recognized IRS-4 or p85 (Fig. 4A). We also confirmed that IRS-4 and p85 bound to the SOCS-6 and SOCS-7 SH2 domains in response to stimulation with serum and insulin (data not shown). Moreover, full-length SOCS-6 but not the N-terminal

TABLE 1. Tandem mass-spectrometric identification of proteins bound to the SOCS-6 and SOCS-7 SH2 domain

Band	Protein identified	Database and accession no.	Mol wt (10^3)	No. of peptides[a]	Sequence coverage (%)
1	IRS-4	TrEMBL, O14654	133.6	15	22.7
2	IRS-2	TrEMBL, Q9Y615	137.7	1	1.3
3	IRS-4	TrEMBL, O14654	133.6	26	33.0
4	PI3K p85 α subunit	SwissProt, P27986	83.5	5	10.4
	PI3K p85 β subunit	SwissProt, O00459	81.6	7	19.5
	IRS-4	TrEMBL, O14654	133.6	5	7.2
5	Tubulin β D1	TIGR human gene index, THC480952	49.7	21	66.7
	Tubulin β-2 chain	SwissProt, P05217	49.8	20	64.9
	Tubulin α-1 chain	SwissProt, P04687	50.1	9	34.8

[a] Number of unique peptides identified.

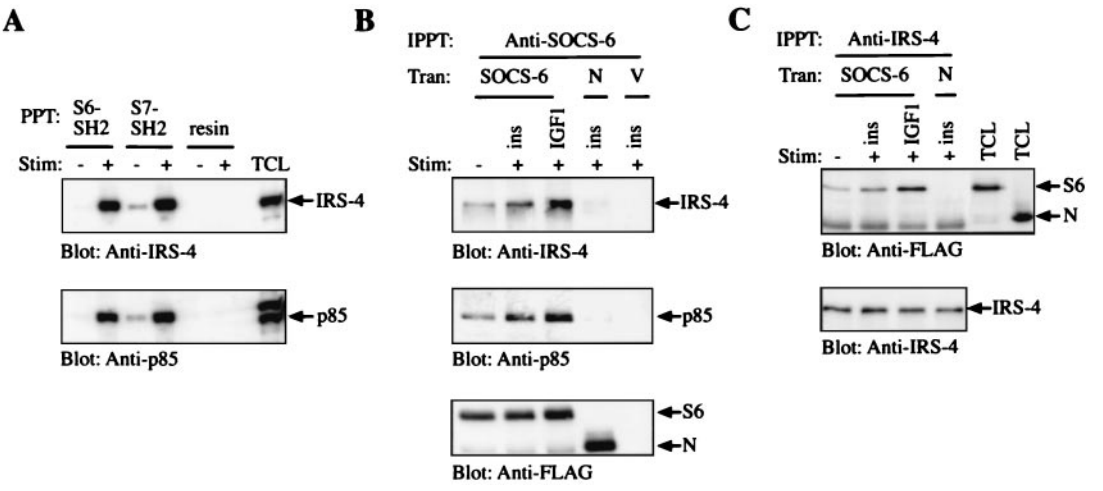

FIG. 4. SOCS-6 associates with IRS-4 and the p85 regulatory subunit of PI3K. (A) 293T cells were either left unstimulated (−) or stimulated (+) with 100 ng of IGF-1 per ml for 15 min. Lysates were subjected to precipitation with either SOCS-6 SH2 resin, SOCS-7 SH2 resin, or control resin, and precipitates were immunoblotted with anti-IRS-4 antibodies (top). The blot was then reprobed with anti-p85 antibodies (bottom). (B) 293T cells were transfected with empty vector (V) or with cDNAs encoding FLAG-S6 or N protein. Cells were either left unstimulated (−) or stimulated (+) with 100 nM insulin (ins) or 100 ng of IGF-1 per ml for 15 min. Lysates were subjected to immunoprecipitation with the 1C3 anti-SOCS-6 antibody (which recognizes the N-terminal region of SOCS-6) followed by immunoblotting with anti-IRS-4 antibodies (top). The blot was then reprobed with anti-p85 antibodies (middle) and anti-FLAG antibodies (bottom). (C) 293T cells were transfected with cDNAs encoding FLAG-S6 or N protein. Cells were either left unstimulated (−) or stimulated (+) with 100 nM insulin (ins) or 100 ng of IGF-1 per ml for 15 min. Lysates were subjected to immunoprecipitation with anti-IRS-4 antibodies followed by immunoblotting with anti-FLAG antibodies (top). The blot was then reprobed with anti-IRS-4 antibodies (bottom). Stim, stimulation; Tran, transfection; IPPT, immunoprecipitate; PPT, precipitate; TCL, total cell lysate.

region of SOCS-6 inducibly associated with IRS-4 and p85 in response to insulin and IGF-1 stimulation (Fig. 4B and C). Interestingly, some IRS-4 was bound to SOCS-6 prior to stimulation, possibly due to a low level of IRS-4 tyrosine phosphorylation in unstimulated cells.

Deletion of the SOCS-6 gene in mice. To assess the physiological role of SOCS-6, we engineered a null mutation in mice by homologous recombination in ES cells. Genomic clones corresponding to two independent SOCS-6 loci were isolated by screening a 129/Sv murine genomic DNA library with oligonucleotides corresponding to the SOCS-6 cDNA sequence. One locus, which represented the functional SOCS-6 gene, contained sequence identical to that of the SOCS-6 cDNA, with the predicted protein-encoding sequence contained on a single exon. The second locus contained a rearranged and truncated version of the SOCS-6 coding exon flanked by sequences unrelated to the first locus. Although this arrangement included an open reading frame corresponding to amino acids 1 to 255 of SOCS-6, an 8-amino-acid deletion and several single amino acid insertions and substitutions were present (data not shown). No transcripts were detectable from this locus, suggesting that it is a nonfunctional pseudogene. A targeting vector was designed to delete the SOCS-6 coding exon of the functional SOCS-6 gene via homologous recombination in ES cells (Fig. 5A).

Chimeric mice derived from each of two targeted ES cell lines were crossed to C57BL/6 mice to generate heterozygous mice, which were then interbred to produce two independent strains of mice harboring the disrupted SOCS-6 gene. The genotypes of all offspring were determined by Southern blot analysis of genomic DNA obtained from tail tips (Fig. 5B). Offspring of heterozygous parents ($n = 171$) included wild-type (SOCS-$6^{+/+}$), heterozygous (SOCS-$6^{+/-}$), and homozygous mutant (SOCS-$6^{-/-}$) mice in numbers consistent with normal Mendelian segregation of the targeted SOCS-6 allele (+/+, 22%; +/−, 57%; −/−, 21%), suggesting that SOCS-6 is not required for embryonic development or postnatal survival. In addition, observation of adult mice lacking the SOCS-6 gene up to 6 months of age revealed that they were viable and fertile and appeared to be indistinguishable from wild-type littermates.

To confirm that SOCS-6 was functionally deleted by this targeting strategy, poly(A)$^+$ RNA was analyzed from tissues obtained from wild-type and SOCS-$6^{-/-}$ mice. SOCS-6 mRNA was expressed in most wild-type tissues, with expression being highest in testes, large intestine, spleen, liver, lung, kidney, thymus, and salivary gland, but was undetectable in all SOCS-$6^{-/-}$ tissues examined (Fig. 5C). Protein lysates were also prepared from a variety of tissues obtained from wild-type and SOCS-$6^{-/-}$ mice. Consistent with analysis of mRNA, SOCS-6 protein was detected in wild-type testes, lung, liver, spleen, heart, and thymus while SOCS-6 protein was not detected in any SOCS-$6^{-/-}$ tissues (Fig. 5D). Together, these experiments confirmed that SOCS-6 is ubiquitously expressed and that the targeted disruption of the SOCS-6 gene resulted in a null allele at this locus.

Mild growth retardation in SOCS-$6^{-/-}$ mice. A comprehensive histological comparison of 17 tissues from each of 39 SOCS-$6^{-/-}$ and 29 wild-type littermate or control C57BL/6 mice aged 10 to 20 weeks revealed no consistent abnormalities in SOCS-$6^{-/-}$ mice. A possible exception was the occurrence of foci of lymphocytes with or without small areas of acinar necrosis in the pancreas in 42% of male SOCS-$6^{-/-}$ mice. In no case did such foci involve islets of Langerhans, which were

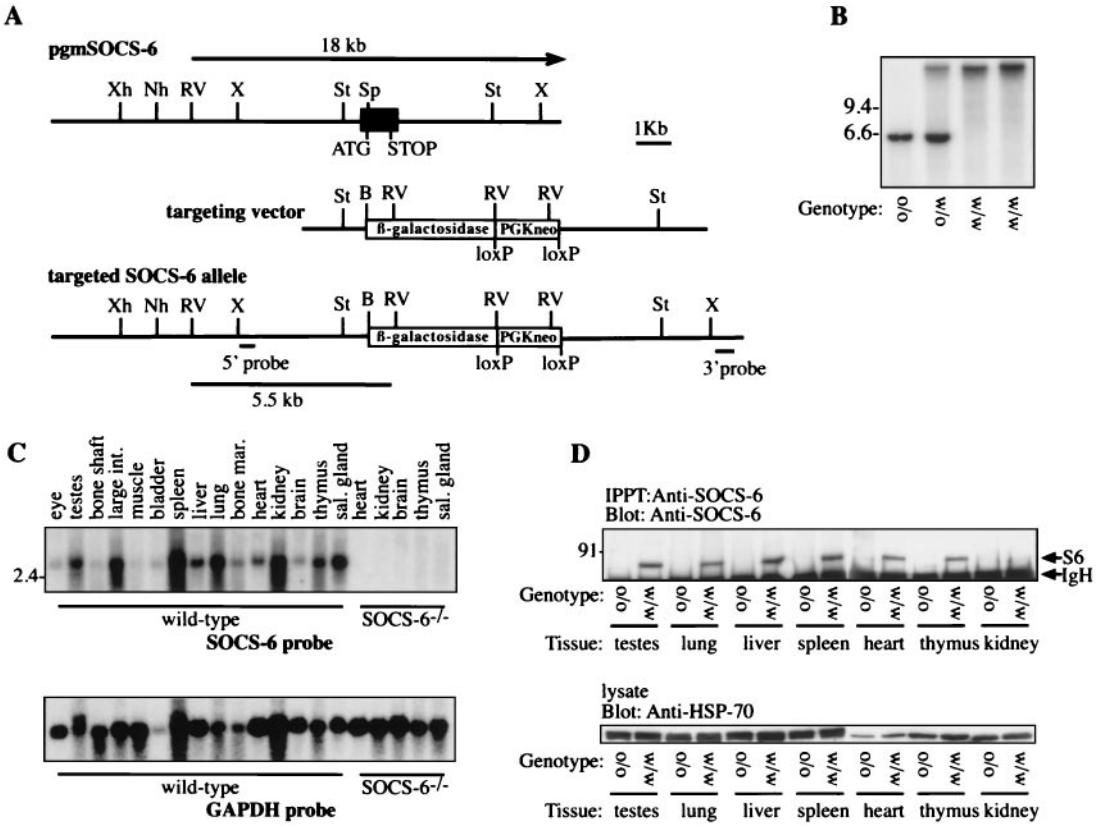

FIG. 5. Disruption of the SOCS-6 gene by homologous recombination. (A) The endogenous SOCS-6 gene is shown (top), with the SOCS-6 coding region depicted as a black box. The targeting vector (middle) was designed so that in the targeted gene (bottom), the SOCS-6 coding exon is replaced by the β-galactosidase PGKneo cassette. (B) Southern blot of *Eco*RV-digested genomic DNA obtained from tail tips of offspring from a cross between SOCS-$6^{+/-}$ mice. The blot was hybridized with a 5′ genomic SOCS-6 probe which distinguished between the endogenous (18-kbp) and the targeted (5.5-kbp) alleles. Sizes (in kilobase pairs) is on the left. (C) Northern blot of poly(A)$^+$ RNA obtained from a variety of wild-type and SOCS-$6^{-/-}$ tissues. The blot was hybridized with a SOCS-6 cDNA probe (top) and then stripped and rehybridized with a GAPDH cDNA probe (bottom) to control for the quality and quantity of mRNA. (D) Western blot analysis of SOCS-6 expression. Lysates from a variety of wild-type and SOCS-$6^{-/-}$ tissues were subjected to immunoprecipitation with anti-SOCS-6 antibody 1C3 followed by immunoblotting with anti-SOCS-6 antibody 3A7 (top). To show that equal amounts of protein were used in each immunoprecipitation, 40 μg of each lysate was analyzed by immunoblotting with an anti-heat shock protein 70 (HSP-70) antibody. Molecular mass (in kilodaltons) is indicated on the left. S6, SOCS-6; IgH, immunoglobulin heavy chain; o/o, SOCS-$6^{-/-}$; w/w, wild-type; w/o, heterozygous; Sal. gland, salivary gland; large int., large intestine.

of normal size and frequency. Although these lesions were more prevalent in SOCS-$6^{-/-}$ mice than in wild-type controls (16%), the increase in prevalence was not statistically significant.

During this analysis, several of the SOCS-$6^{-/-}$ mice appeared to be slightly smaller than wild-type littermates. To formally examine growth of SOCS-$6^{-/-}$ mice, offspring from SOCS-$6^{+/-}$ crosses were weighed weekly from weaning until 14 weeks of age. The weights of both male and female SOCS-$6^{-/-}$ mice were no different from sex-matched littermate controls until 4 weeks of age. However, from 5 weeks of age the SOCS-$6^{-/-}$ mice consistently weighed 8 to 10% less than their wild-type littermates at all ages examined (Fig. 6).

Hematological parameters in SOCS-$6^{-/-}$ mice. Northern blotting data suggested that SOCS-6 was expressed in hematopoietic tissues. To further define SOCS-6 expression in hematopoietic cells, we took advantage of the incorporation of the *lacZ* marker gene into the targeted SOCS-6 locus. Using β-galactosidase expression as a surrogate for SOCS-6 in flow-cytometric analysis, we confirmed SOCS-6 transcription in bone marrow cells. Comparison of the *lacZ* staining profile from SOCS-$6^{-/-}$ mice with that from wild-type controls showed that a majority of cells exhibited high or medium staining, indicating that SOCS-6 is transcribed by most cells in the bone marrow (Fig. 7). The cells in the highly stained fraction were slightly enriched in monocytes and immature granulocytes compared with low-staining populations, but all cell types were present in both fractions (data not shown). Culture of high, medium, and low LacZ-staining fractions indicated that most progenitor cells in the granulocyte, macrophage, eosinophil, and megakaryocytic lineages also expressed SOCS-6 (Table 2).

The prominent expression of SOCS-6 in the hematopoietic compartment prompted examination of hematopoiesis in 12 adult SOCS-$6^{-/-}$ mice. However, no anomaly in the numbers of circulating white blood cells or platelets was evident, nor were differences observed in hematocrit levels or total femoral bone marrow cell counts. The frequencies of morphologically recognizable cell types in the peritoneal cavity, spleen, and bone marrow were also normal in SOCS-$6^{-/-}$ mice (Table 3),

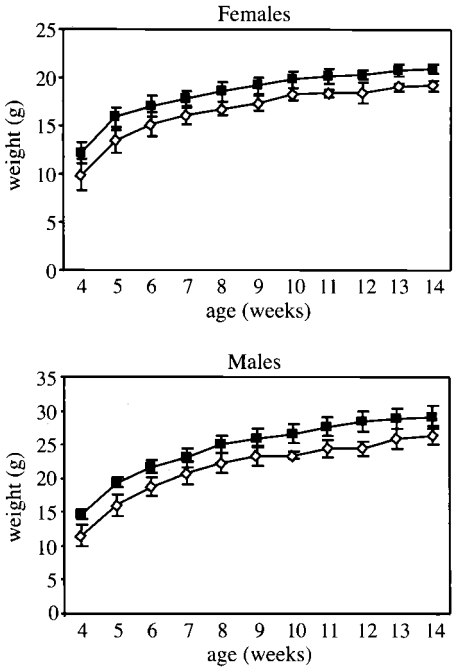

FIG. 6. Growth curves of SOCS-$6^{-/-}$ mice and wild-type littermates. Data are from 14 litters and represent 10 wild-type males, 7 SOCS-$6^{-/-}$ males, 16 wild-type females, and 8 SOCS-$6^{-/-}$ females. Values are means ± standard deviations. Open triangles, SOCS-$6^{-/-}$ mice; closed squares, SOCS-$6^{+/+}$ mice. $P < 0.05$ at all points.

as were the numbers and lineage commitment of hematopoietic progenitor cells in the bone marrow assayed in clonal cultures (data not shown). Finally, FACS analysis of the thymus, spleen, mesenteric node, and bone marrow revealed no abnormalities in the frequency of T and B lymphocytes, macrophages, granulocytes, or erythroid cells (data not shown).

Blood glucose and plasma insulin levels in SOCS-$6^{-/-}$ mice. Our finding that SOCS-6 bound to IRS-2 and IRS-4 in response to insulin stimulation together with a recent report that

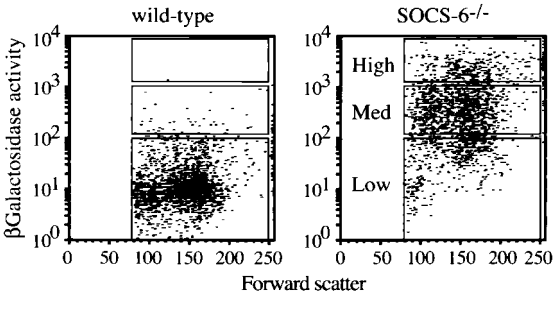

FIG. 7. β-Galactosidase expression in bone marrow cells from wild-type and SOCS-$6^{-/-}$ mice. The β-galactosidase gene was "knocked in" to the targeted SOCS-6 locus and could therefore be used as a surrogate for SOCS-6 expression in SOCS-$6^{-/-}$ cells. Bone marrow cells were loaded by incubation with fluorescein-di-β-D-galactopyranoside under hypotonic conditions and then analyzed by flow cytometry. Cells were sorted into three fractions, designated high, medium (med), and low, which represented 21, 45, and 24% of the total population, respectively. The remaining 10% of cells did not lie within these fractions.

TABLE 2. Distribution of β-galactosidase-positive progenitor cells in the bone marrow of SOCS-$6^{-/-}$ mice

Stimulus	β-Galactosidase activity	% Distribution[a]					
		Blast	G	GM	M	Eo	Meg
GM-CSF	Low		4	0	3	10	
	Medium		47	18	20	33	
	High		48	82	77	57	
IL-3	Low	0	2	4	7	0	13
	Medium	64	58	42	46	88	78
	High	36	40	54	47	12	9
G-CSF + SCF	Low	4	9	12	18		
	Medium	35	40	20	12		
	High	61	51	68	71		

[a] Values are the percentages in each FACSgal fraction of the combined total number of colonies of each lineage present in the fractions. G, granulocytic; GM, granulocyte-macrophage; M, macrophage; Eo, eosinophil; Meg, megakaryocyte.

SOCS-6 interacts with and inhibits signaling from the insulin receptor (29) led us to examine insulin signaling in SOCS-$6^{-/-}$ mice. To investigate whether glucose homeostasis was perturbed by the absence of SOCS-6, we measured plasma insulin and blood glucose concentrations in SOCS-$6^{-/-}$ and wild-type mice, in both the fasting and fed states. We found that there were no significant differences in glucose or insulin concentrations ($P < 0.01$) between SOCS-$6^{-/-}$ and wild-type mice, suggesting that glucose homeostasis was not perturbed in SOCS-$6^{-/-}$ animals (Fig. 8A and B).

Glucose and insulin tolerance tests. To investigate further glucose homeostasis in SOCS-$6^{-/-}$ mice, we carried out glucose and insulin tolerance tests. We reasoned that if SOCS-6 was a negative regulator of insulin signaling, insulin action should be enhanced in SOCS-$6^{-/-}$ mice. We found that SOCS-$6^{-/-}$ mice did not demonstrate an enhanced or sustained clearance of glucose in response to glucose or insulin injection, compared to wild-type mice (Fig. 8C and D). This suggested that SOCS-$6^{-/-}$ tissues were not hyperresponsive to the insulin that was directly injected or released in response to glucose injection. Thus, SOCS-$6^{-/-}$ mice did not appear to be more insulin responsive than wild type mice.

Expression pattern of SOCS-7. Mooney et al. (29) recently reported that SOCS-6 inhibits insulin signaling when overexpressed in cell lines; however, our results suggested that SOCS-6 was not critical in the regulation of glucose homeostasis in vivo. One possibility is that SOCS-7 might compensate for SOCS-6 action in the absence of SOCS-6. To examine the expression pattern of SOCS-7 and to determine whether the expression of SOCS-7 is altered in mice that lack SOCS-6, we carried out Northern blot analysis of poly(A)$^+$ RNA obtained from a panel of wild-type and SOCS-$6^{-/-}$ tissues. We found that SOCS-7 mRNA was expressed in most wild-type tissues, with expression being highest in testes, brain, and spleen. In addition, the expression of SOCS-7 was not altered in SOCS-$6^{-/-}$ tissues (Fig. 9).

DISCUSSION

We have used biochemical and biological approaches to investigate the action of SOCS-6. We found that SOCS-6 was

TABLE 3. Hematology parameters in SOCS-6$^{-/-}$ mice and wild-type littermates

Parameter	Value for mice[a]	
	SOCS-6$^{-/-}$ (n = 12)	SOCS-6$^{+/+}$ (n = 9)
No. of peripheral white cells/μl		
Total	7,600 ± 3,150	7,450 ± 2,620
Neutrophils	980 ± 770	770 ± 520
Lymphocytes	5,960 ± 2,320	6,120 ± 1,970
Monocytes	520 ± 440	420 ± 230
Eosinophils	160 ± 120	140 ± 140
No. of platelets/μl	878,230 ± 147,460	906,190 ± 132,910
Hematocrit (%)	44 ± 2	45 ± 1
Spleen		
Wt (mg)	82 ± 18	85 ± 21
Blasts (%)	2 ± 1	3 ± 2
Myelocytes (%)	0.2 ± 0.6	0.3 ± 0.7
Neutrophils (%)	3 ± 3	4 ± 3
Lymphocytes (%)	87 ± 6	84 ± 8
Monocytes (%)	2 ± 1	2 ± 1
Eosinophils (%)	0.6 ± 0.8	0.7 ± 0.7
Nucleated RBC (%)[b]	5 ± 3	7 ± 5
Marrow		
No. of cells/femur (10^6)	38.9 ± 4.0	40.5 ± 6.0
Blasts (%)	1.4 ± 0.6	1.1 ± 0.7
Myelocytes (%)	3.0 ± 0.9	3.8 ± 1.7
Neutrophils (%)	14.0 ± 4.2	14.5 ± 2.9
Lymphocytes (%)	7.9 ± 2.4	7.4 ± 1.9
Monocytes (%)	3.3 ± 0.9	2.6 ± 1.0
Eosinophils (%)	1.3 ± 0.8	1.3 ± 0.7
Nucleated RBC	8.0 ± 2.1	9.9 ± 2.6
Peritoneal cavity		
Total cells (10^6)	9.7 ± 3.6	6.2 ± 2.3
Neutrophils (10^6)	0	0
Lymphocytes (10^6)	4.1 ± 1.7	2.1 ± 0.9
Macrophages (10^6)	5.4 ± 2.2	3.9 ± 1.5
Eosinophils (10^6)	0.06 ± 0.14	0.03 ± 0.04
Mast cells (10^6)	0.14 ± 0.10	0.15 ± 0.10

[a] Values are means ± standard deviations.
[b] RBC, red blood cells.

ubiquitously expressed during embryonic development (data not shown) and in the adult mouse and that SOCS-6 constitutively bound to the elongin B/C complex in a SOCS box-dependent manner. It is therefore probable that SOCS-6, like other SOCS box-containing proteins, acts as an adapter that targets proteins bound to its SH2 domain for ubiquitination and destruction by the proteasome.

An investigation of the SOCS-6 and SOCS-7 SH2 domain binding specificity revealed that both SH2 domains preferentially bound to phosphopeptides containing a valine in the pY +1 position and a hydrophobic residue in the pY +2 or pY +3 position. The binding preferences were very similar, as might be anticipated from the high degree of sequence homology between the two SH2 domains, particularly within the ligand-binding pocket. We used the SOCS-6 and SOCS-7 SH2 domains as affinity reagents to purify proteins from lysates derived from IGF-1-stimulated cells and found that the prominent binding partners were IRS-2, IRS-4, and the p85 regulatory subunit of PI3K (p85α and p85β). We also confirmed that full-length SOCS-6 bound to IRS-4 and p85 in response to stimulation with either insulin or IGF-1.

IRS-2 and IRS-4 are members of the IRS family (IRS-1 to IRS-4), which are tyrosine phosphorylated on 8 to 18 sites following insulin or IGF-1 stimulation and form signaling complexes at the receptor with SH2 domain-containing proteins, including the p85 regulatory subunit of PI3K, Grb2, Nck, and SHP2 (4). In this way, IRS family members act as docking proteins that amplify insulin and IGF-1-induced signaling cascades. IRS proteins therefore play a key role in the regulation of growth and metabolism (4, 12).

It is likely that SOCS-6 binds directly to IRS-4, as IRS-4 is tyrosine phosphorylated on multiple sites in response to insulin or IGF-1 stimulation and contains a total of four Tyr-Val-X-hydrophobic motifs (Y700, Y828, Y921, and Y959) and one Tyr-Val-hydrophobic-X motif (Y1046). The SOCS-6 SH2 domain weakly precipitated IRS-2, which contains one potential SOCS-6 SH2 domain binding site (Y823). P85β also contains one potential SOCS-6 SH2 domain binding site (Y74, which lies within the p85β SH3 domain) while p85α does not. However, p85 is not reported to be tyrosine phosphorylated, and it is therefore unlikely to bind directly to the SOCS-6 SH2 domain. Given that p85 is a very prominent IRS-binding protein (12), it is likely that p85 associates indirectly with SOCS-6 via IRS-4 or IRS-2.

Mooney et al. (29) recently reported that SOCS-6 associates with the insulin receptor in response to insulin stimulation. Our finding that SOCS-6 associated with IRS-2 and IRS-4 suggests that SOCS-6 might interact with the insulin receptor indirectly, via IRS family members. It is unlikely that SOCS-6 binds directly to the insulin receptor through its SH2 domain, as neither the human nor mouse insulin receptor β chain contains a potential SOCS-6 SH2 domain binding site in its cytoplasmic domain. SOCS-6 was found to inhibit the insulin-induced activation of Akt, Erk1/2, and IRS-1, although the mechanism of SOCS-6 action was unknown (29). Our data raise the possibility that SOCS-6 could block access of SH2 domain-containing proteins to phosphotyrosine binding sites on IRS proteins. In this way, SOCS-6 could prevent the recruitment of signaling proteins to the receptor complex and thereby inhibit their activation. In addition, SOCS-6 might stimulate the proteasomal degradation of the insulin receptor complex by recruiting the ubiquitin ligase machinery through its SOCS box.

To investigate the biological action of SOCS-6, we generated mice that lacked the SOCS-6 gene. We found that hematopoiesis in SOCS-6$^{-/-}$ mice was indistinguishable from that in wild-type littermates, despite that fact that SOCS-6 was expressed in progenitor cells and hematopoietic tissues. In addition, a histological examination of 17 tissues revealed that there were no significant differences between the tissues of wild-type and SOCS-6$^{-/-}$ mice.

The fact that SOCS-6 associated with IRS-4, IRS-2, and the insulin receptor and inhibited insulin signaling in vitro led us to examine insulin signaling in vivo. A key function of insulin is to stimulate the uptake of glucose by insulin-sensitive tissues such as liver, muscle, and fat (5). As a consequence, mice lacking negative regulators of the insulin signaling pathway such as the phosphatases SHIP2 and PTP1B exhibit reduced levels of

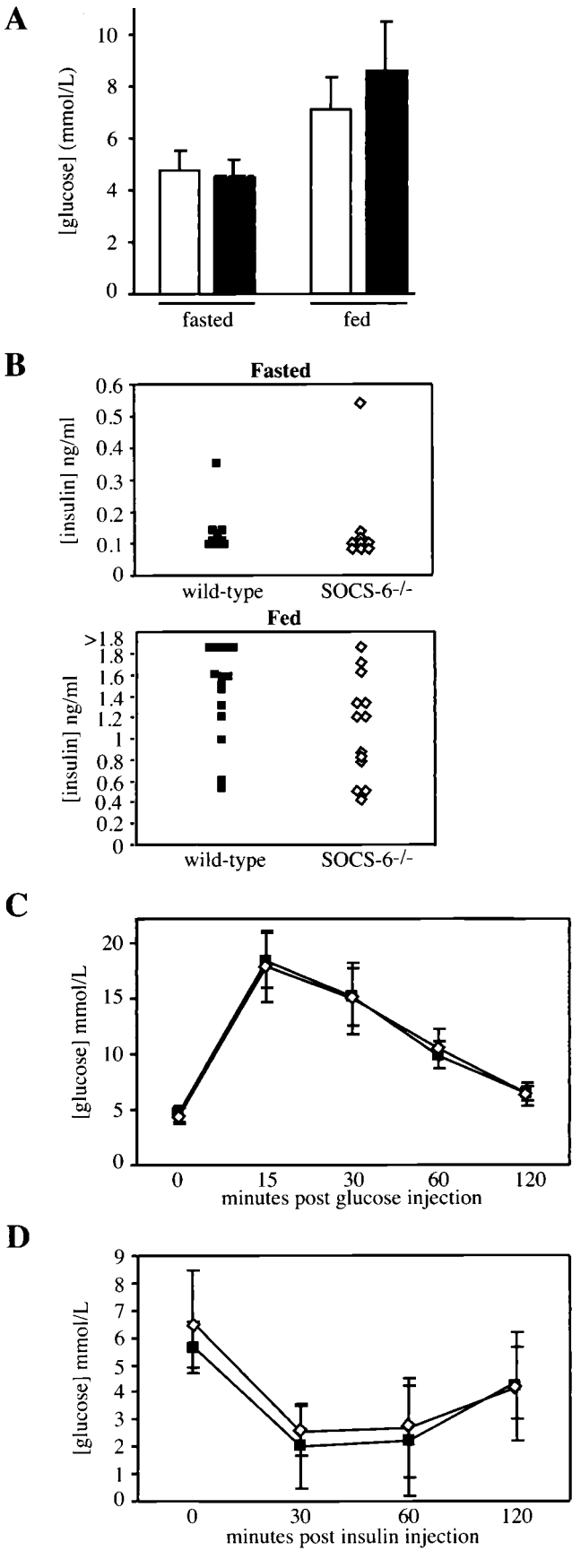

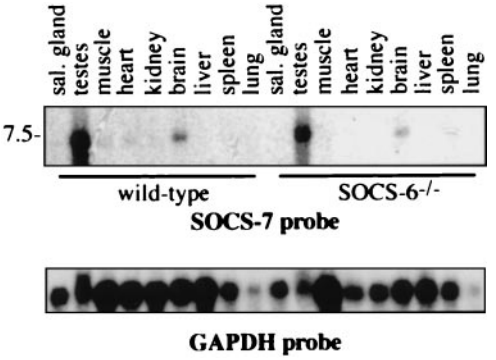

FIG. 9. Expression pattern of SOCS-7. Poly(A)$^+$ RNA was obtained from a variety of wild-type and SOCS-6$^{-/-}$ tissues and subjected to Northern blot analysis. The blot was hybridized with a SOCS-7 cDNA probe (top) and then stripped and rehybridized with a GAPDH cDNA probe (bottom) to control for the quality and quantity of mRNA. Sal. gland, salivary gland.

blood glucose, as well as an enhanced ability to clear glucose in response to an insulin or glucose challenge (6, 9). We found that SOCS-6$^{-/-}$ mice did not exhibit reduced glucose levels or enhanced glucose clearance in response to the administration of glucose or insulin, suggesting that they were not insulin hyperresponsive. One possibility was that SOCS-6$^{-/-}$ mice might have compensated for enhanced insulin sensitivity by lowering their plasma insulin levels; however, we could not detect a difference in plasma insulin concentrations between wild-type and SOCS-6$^{-/-}$ mice. Thus, although SOCS-6 has been reported to inhibit insulin signaling when overexpressed, it did not appear to be critical in the regulation of glucose homeostasis in vivo.

One possible explanation is that other SOCS family members can compensate for SOCS-6 action in the absence of SOCS-6. For example, SOCS-1 negatively regulates insulin signaling, both in vitro (29) and in vivo (19), and therefore could potentially compensate for the lack of SOCS-6. Similarly, our finding that the SOCS-7 SH2 domain also bound to IRS proteins suggests that SOCS-6 and SOCS-7 might have overlapping actions. The fact that SOCS-6 and SOCS-7 are both expressed in many tissues supports this possibility. However, we found that SOCS-7 mRNA was not upregulated in SOCS-6$^{-/-}$ mice, suggesting that compensation, if present,

FIG. 8. Glucose homeostasis in wild-type and SOCS-6$^{-/-}$ mice. (A) Blood glucose levels were determined for male wild-type (filled bars) or SOCS-6$^{-/-}$ (open bars) mice that either fasted overnight (n = 20) or were fed ad libitum (n = 13 to 15). Mice were 7 to 10 weeks old. (B) Plasma insulin levels were determined for male wild-type or SOCS-6$^{-/-}$ mice that either fasted overnight or were fed ad libitum. Mice were 7 to 11 weeks old. (C) Glucose tolerance test. Male wild-type (closed squares) and SOCS-6$^{-/-}$ (open triangles) mice (n = 10) fasted overnight and then received an intraperitoneal injection of 1.2 g of D-glucose per kg of body weight. Blood glucose levels were determined at the indicated time points. Mice were 9 to 10 weeks old. (D) Insulin tolerance test. Male wild-type (closed squares) and SOCS-6$^{-/-}$ (open triangles) mice (n = 10) fasted overnight and were then subjected to an intraperitoneal injection of 0.75 U of insulin per kg of body weight. Blood glucose levels were determined at the indicated intervals. Mice were 16 to 18 weeks old.

would presumably occur at a normal expression level of SOCS-7.

The major difference between SOCS-6$^{-/-}$ and wild-type mice was that SOCS-6$^{-/-}$ mice exhibited an 8 to 10% reduction in body weight. Mice lacking SOCS-2 also exhibit dysregulated growth, likely due to perturbation of the GH/IGF-1 axis. The fact that SOCS-6 binds to IRS family members in response to IGF-1 stimulation suggests that SOCS-6 might also modulate IGF-1 signaling, although its role remains unclear. Interestingly, insulin signaling in the brain has been implicated in the regulation of food intake and body weight. Injections of insulin inhibit food intake and reduce body weight in a dose-dependent manner (40). In addition, female mice with a brain-specific disruption of the insulin receptor exhibit an increase in body weight and food intake, while both male and female mice lacking brain insulin receptor exhibit diet-sensitive obesity (3). Thus, although it appears that SOCS-6 is dispensable in the regulation of glucose homeostasis by "insulin-sensitive" tissues, such as liver, muscle, and fat, it is possible that SOCS-6 regulates insulin signaling in "insulin-insensitive tissues," like the brain. If this is the case, a lack of SOCS-6 might result in enhanced insulin signaling and a corresponding reduction in food intake and body weight. We are currently investigating this possibility.

ACKNOWLEDGMENTS

This work was supported by the National Health and Medical Research Council, Canberra, Australia; the Anti-Cancer Council of Victoria; the National Institutes of Health, Bethesda, Md., grant CA22556; the J. D. and L. Harris Trust; the Australian Federal Government Cooperative Research Centres Program; and AMRAD Operations Pty. Ltd., Melbourne, Australia. D.L.K. is the recipient of a University of Melbourne Overseas Postgraduate Award.

We thank Ken Harder for helpful discussions and Wendy Carter, Tracy Willson, and Maria Asimakis for work involved in the production of monoclonal antibodies. We also thank Adrian Batchelor and Charles E. Stebbins for providing the pBB75 and pGEX4T3-elongin B plasmids, respectively.

REFERENCES

1. **Alexander, W. S., D. Metcalf, and A. R. Dunn.** 1995. Point mutations within a dimer interface homology domain of c-Mpl induce constitutive receptor activity and tumorigenicity. EMBO J. **14:**5569–5578.
2. **Alexander, W. S., R. Starr, J. E. Fenner, C. L. Scott, E. Handman, N. S. Sprigg, J. E. Corbin, A. L. Cornish, R. Darwiche, C. M. Owczarek, T. W. Kay, N. A. Nicola, P. J. Hertzog, D. Metcalf, and D. J. Hilton.** 1999. SOCS1 is a critical inhibitor of interferon gamma signaling and prevents the potentially fatal neonatal actions of this cytokine. Cell **98:**597–608.
3. **Bruning, J. C., D. Gautam, D. J. Burks, J. Gillette, M. Schubert, P. C. Orban, R. Klein, W. Krone, D. Muller-Wieland, and C. R. Kahn.** 2000. Role of brain insulin receptor in control of body weight and reproduction. Science **289:**2122–2125.
4. **Burks, D. J., and M. F. White.** 2001. IRS proteins and beta-cell function. Diabetes **50**(Suppl. 1)**:**S140-S145.
5. **Cefalu, W. T.** 2001. Insulin resistance: cellular and clinical concepts. Exp. Biol. Med. (Maywood) **226:**13–26.
6. **Clement, S., U. Krause, F. Desmedt, J. F. Tanti, J. Behrends, X. Pesesse, T. Sasaki, J. Penninger, M. Doherty, W. Malaisse, J. E. Dumont, Y. Le Marchand-Brustel, C. Erneux, L. Hue, and S. Schurmans.** 2001. The lipid phosphatase SHIP2 controls insulin sensitivity. Nature **409:**92–97.
7. **Cohney, S. J., D. Sanden, N. A. Cacalano, A. Yoshimura, A. Mui, T. S. Migone, and J. A. Johnston.** 1999. SOCS-3 is tyrosine phosphorylated in response to interleukin-2 and suppresses STAT5 phosphorylation and lymphocyte proliferation. Mol. Cell. Biol. **19:**4980–4988.
8. **De Sepulveda, P., S. Ilangumaran, and R. Rottapel.** 2000. Suppressor of cytokine signaling-1 inhibits VAV function through protein degradation. J. Biol. Chem. **275:**14005–14008.
9. **Elchebly, M., P. Payette, E. Michaliszyn, W. Cromlish, S. Collins, A. L. Loy, D. Normandin, A. Cheng, J. Himms-Hagen, C. C. Chan, C. Ramachandran, M. J. Gresser, M. L. Tremblay, and B. P. Kennedy.** 1999. Increased insulin sensitivity and obesity resistance in mice lacking the protein tyrosine phosphatase-1B gene. Science **283:**1544–1548.
10. **Elefanty, A. G., C. G. Begley, D. Metcalf, L. Barnett, F. Kontgen, and L. Robb.** 1998. Characterization of hematopoietic progenitor cells that express the transcription factor SCL, using a lacZ "knock-in" strategy. Proc. Natl. Acad. Sci. USA **95:**11897–11902.
11. **Frantsve, J., J. Schwaller, D. W. Sternberg, J. Kutok, and D. G. Gilliland.** 2001. Socs-1 inhibits TEL-JAK2-mediated transformation of hematopoietic cells through inhibition of JAK2 kinase activity and induction of proteasome-mediated degradation. Mol. Cell. Biol. **21:**3547–3557.
12. **Giovannone, B., M. L. Scaldaferri, M. Federici, O. Porzio, D. Lauro, A. Fusco, P. Sbraccia, P. Borboni, R. Lauro, and G. Sesti.** 2000. Insulin receptor substrate (IRS) transduction system: distinct and overlapping signaling potential. Diabetes Metab. Res. Rev. **16:**434–441.
13. **Hanada, T., T. Yoshida, I. Kinjyo, S. Minoguchi, H. Yasukawa, S. Kato, H. Mimata, Y. Nomura, Y. Seki, M. Kubo, and A. Yoshimura.** 2001. A mutant form of JAB/SOCS1 augments the cytokine-induced JAK/STAT pathway by accelerating degradation of wild-type JAB/CIS family proteins through the SOCS-box. J. Biol. Chem. **276:**40746–40754.
14. **Hansen, J. A., K. Lindberg, D. J. Hilton, J. H. Nielsen, and N. Billestrup.** 1999. Mechanism of inhibition of growth hormone receptor signaling by suppressor of cytokine signaling proteins. Mol. Endocrinol. **13:**1832–1843.
15. **Helman, D., Y. Sandowski, Y. Cohen, A. Matsumoto, A. Yoshimura, S. Merchav, and A. Gertler.** 1998. Cytokine-inducible SH2 protein (CIS3) and JAK2 binding protein (JAB) abolish prolactin receptor-mediated STAT5 signaling. FEBS Lett. **441:**287–291.
16. **Kamizono, S., T. Hanada, H. Yasukawa, S. Minoguchi, R. Kato, M. Minoguchi, K. Hattori, S. Hatakeyama, M. Yada, S. Morita, T. Kitamura, H. Kato, K. Nakayama, and A. Yoshimura.** 2001. The SOCS box of SOCS-1 accelerates ubiquitin-dependent proteolysis of TEL-JAK2. J. Biol. Chem. **276:**12530–12538.
17. **Kamura, T., D. Burian, Q. Yan, S. L. Schmidt, W. S. Lane, E. Querido, P. E. Branton, A. Shilatifard, R. C. Conaway, and J. W. Conaway.** 2001. MUF1, a novel elongin BC-interacting leucine-rich repeat protein that can assemble with Cul5 and Rbx1 to reconstitute a ubiquitin ligase. J. Biol. Chem. **276:**29748–29753.
18. **Kamura, T., S. Sato, D. Haque, L. Liu, W. G. Kaelin, Jr., R. C. Conaway, and J. W. Conaway.** 1998. The elongin BC complex interacts with the conserved SOCS-box motif present in members of the SOCS, ras, WD-40 repeat, and ankyrin repeat families. Genes Dev. **12:**3872–3881.
19. **Kawazoe, Y., T. Naka, M. Fujimoto, H. Kohzaki, Y. Morita, M. Narazaki, K. Okumura, H. Saitoh, R. Nakagawa, Y. Uchiyama, S. Akira, and T. Kishimoto.** 2001. Signal transducer and activator of transcription (STAT)-induced STAT inhibitor 1 (SSI-1)/suppressor of cytokine signaling 1 (SOCS1) inhibits insulin signal transduction pathway through modulating insulin receptor substrate 1 (IRS-1) phosphorylation. J. Exp. Med. **193:**263–269.
20. **Kile, B. T., D. Metcalf, S. Mifsud, L. DiRago, N. A. Nicola, D. J. Hilton, and W. S. Alexander.** 2001. Functional analysis of Asb-1 using genetic modification in mice. Mol. Cell. Biol. **21:**6189–6197.
21. **Kontgen, F., and C. L. Stewart.** 1993. Simple screening procedure to detect gene targeting events in embryonic stem cells. Methods Enzymol. **225:**878–890.
22. **Krebs, D. L., and D. J. Hilton.** 2000. SOCS: physiological suppressors of cytokine signaling. J. Cell Sci. **113:**2813–2819.
23. **Marine, J. C., C. McKay, D. Wang, D. J. Topham, E. Parganas, H. Nakajima, H. Pendeville, H. Yasukawa, A. Sasaki, A. Yoshimura, and J. N. Ihle.** 1999. SOCS3 is essential in the regulation of fetal liver erythropoiesis. Cell **98:**617–627.
24. **Marine, J. C., D. J. Topham, C. McKay, D. Wang, E. Parganas, D. Stravopodis, A. Yoshimura, and J. N. Ihle.** 1999. SOCS1 deficiency causes a lymphocyte-dependent perinatal lethality. Cell **98:**609–616.
25. **Masuhara, M., H. Sakamoto, A. Matsumoto, R. Suzuki, H. Yasukawa, K. Mitsui, T. Wakioka, S. Tanimura, A. Sasaki, H. Misawa, M. Yokouchi, M. Ohtsubo, and A. Yoshimura.** 1997. Cloning and characterization of novel CIS family genes. Biochem. Biophys. Res. Commun. **239:**439–446.
26. **Matuoka, K., H. Miki, K. Takahashi, and T. Takenawa.** 1997. A novel ligand for an SH3 domain of the adaptor protein Nck bears an SH2 domain and nuclear signaling motifs. Biochem. Biophys. Res. Commun. **239:**488–492.
27. **Metcalf, D., C. J. Greenhalgh, E. Viney, T. A. Willson, R. Starr, N. A. Nicola, D. J. Hilton, and W. S. Alexander.** 2000. Gigantism in mice lacking suppressor of cytokine signalling-2. Nature **405:**1069–1073.
28. **Monni, R., S. C. Santos, M. Mauchauffe, R. Berger, J. Ghysdael, F. Gouilleux, S. Gisselbrecht, O. Bernard, and V. Penard-Lacronique.** 2001. The TEL-Jak2 oncoprotein induces Socs1 expression and altered cytokine response in Ba/F3 cells. Oncogene **20:**849–858.
29. **Mooney, R. A., J. Senn, S. Cameron, N. Inamdar, L. M. Boivin, Y. Shang, and R. W. Furlanetto.** 2001. Suppressors of cytokine signaling-1 and -6 associate with and inhibit the insulin receptor. A potential mechanism for cytokine-mediated insulin resistance. J. Biol. Chem. **276:**25889–25893.
30. **Naka, T., T. Matsumoto, M. Narazaki, M. Fujimoto, Y. Morita, Y. Ohsawa, H. Saito, T. Nagasawa, Y. Uchiyama, and T. Kishimoto.** 1998. Accelerated apoptosis of lymphocytes by augmented induction of Bax in SSI-1 (STAT-

induced STAT inhibitor-1) deficient mice. Proc. Natl. Acad. Sci. USA **95:** 15577–15582.
31. **Nicholson, S. E., T. A. Willson, A. Farley, R. Starr, J. G. Zhang, M. Baca, W. S. Alexander, D. Metcalf, D. J. Hilton, and N. A. Nicola.** 1999. Mutational analyses of the SOCS proteins suggest a dual domain requirement but distinct mechanisms for inhibition of LIF and IL-6 signal transduction. EMBO J. **18:**375–385.
32. **Pezet, A., H. Favre, P. A. Kelly, and M. Edery.** 1999. Inhibition and restoration of prolactin signal transduction by suppressors of cytokine signaling. J. Biol. Chem. **274:**24497–24502.
33. **Ram, P. A., and D. J. Waxman.** 2000. Role of the cytokine-inducible SH2 protein CIS in desensitization of STAT5b signaling by continuous growth hormone. J. Biol. Chem. **275:**39487–39496.
34. **Ram, P. A., and D. J. Waxman.** 1999. SOCS/CIS protein inhibition of growth hormone-stimulated STAT5 signaling by multiple mechanisms. J. Biol. Chem. **274:**35553–35561.
35. **Roberts, A. W., L. Robb, S. Rakar, L. Hartley, L. Cluse, N. A. Nicola, D. Metcalf, D. J. Hilton, and W. S. Alexander.** 2001. Placental defects and embryonic lethality in mice lacking suppressor of cytokine signaling 3. Proc. Natl. Acad. Sci. USA **98:**9324–9329.
36. **Sasaki, A., H. Yasukawa, A. Suzuki, S. Kamizono, T. Syoda, I. Kinjyo, M. Sasaki, J. A. Johnston, and A. Yoshimura.** 1999. Cytokine-inducible SH2 protein-3 (CIS3/SOCS3) inhibits Janus tyrosine kinase by binding through the N-terminal kinase inhibitory region as well as SH2 domain. Genes Cells **4:**339–351.
37. **Starr, R., D. Metcalf, A. G. Elefanty, M. Brysha, T. A. Willson, N. A. Nicola, D. J. Hilton, and W. S. Alexander.** 1998. Liver degeneration and lymphoid deficiencies in mice lacking suppressor of cytokine signaling-1. Proc. Natl. Acad. Sci. USA **95:**14395–14399.
38. **Starr, R., T. A. Willson, E. M. Viney, L. J. Murray, J. R. Rayner, B. J. Jenkins, T. J. Gonda, W. S. Alexander, D. Metcalf, N. A. Nicola, and D. J. Hilton.** 1997. A family of cytokine-inducible inhibitors of signalling. Nature **387:**917–921.
39. **Strasser, A., A. W. Harris, and S. Cory.** 1991. bcl-2 transgene inhibits T cell death and perturbs thymic self-censorship. Cell **67:**889–899.
40. **Woods, S. C., R. J. Seeley, D. Porte, Jr., and M. W. Schwartz.** 1998. Signals that regulate food intake and energy homeostasis. Science **280:**1378–1383.
41. **Yasukawa, H., H. Misawa, H. Sakamoto, M. Masuhara, A. Sasaki, T. Wakioka, S. Ohtsuka, T. Imaizumi, T. Matsuda, J. N. Ihle, and A. Yoshimura.** 1999. The JAK-binding protein JAB inhibits Janus tyrosine kinase activity through binding in the activation loop. EMBO J. **18:**1309–1320.
42. **Yoshimura, A., T. Ohkubo, T. Kiguchi, N. A. Jenkins, D. J. Gilbert, N. G. Copeland, T. Hara, and A. Miyajima.** 1995. A novel cytokine-inducible gene CIS encodes an SH2-containing protein that binds to tyrosine-phosphorylated interleukin 3 and erythropoietin receptors. EMBO J. **14:**2816–2826.
43. **Zhang, J. G., A. Farley, S. E. Nicholson, T. A. Willson, L. M. Zugaro, R. J. Simpson, R. L. Moritz, D. Cary, R. Richardson, G. Hausmann, B. J. Kile, S. B. Kent, W. S. Alexander, D. Metcalf, D. J. Hilton, N. A. Nicola, and M. Baca.** 1999. The conserved SOCS box motif in suppressors of cytokine signaling binds to elongins B and C and may couple bound proteins to proteasomal degradation. Proc. Natl. Acad. Sci. USA **96:**2071–2076.
44. **Zong, C. S., J. Chan, D. E. Levy, C. Horvath, H. B. Sadowski, and L. H. Wang.** 2000. Mechanism of STAT3 activation by insulin-like growth factor I receptor. J. Biol. Chem. **275:**15099–15105.